Observations of Tilting Meddies*

DAVID WALSH,+ PHILIP L. RICHARDSON, AND JIM LYNCH

Woods Hole Oceanographic Institution, Woods Hole, Massachusetts

(Manuscript received 25 April 1995, in final form 23 October 1995)

ABSTRACT

SOFAR floats at different depths within two Mediterranean Water eddies (meddies) reveal that the meddy rotation axes tilt transversely with respect to the meddy translation direction. The rotation axis of one of the meddies (Meddy 1) was displaced by about 6 km over a depth of roughly 100 m; the axis of the second meddy (Meddy 2) was displaced by about 0.4 km over 100-m depth. These results are compared to a simple theoretical model that predicts the deformation and translation of a lens-shaped eddy embedded in large-scale external shear. Observed lateral deformations of the meddies are in good agreement with model predictions. The observed tilt of Meddy 1 is attributed to a combination of depth-varying rotation rate beneath the meddy core and the horizontal translation of the meddy; the tilt of Meddy 2 is attributed to a deformation of the meddy core by vertically sheared flow outside the meddy. The observed translation speed of the meddies with respect to nearby floats outside of the meddies is significantly larger than that predicted by the model.

1. Introduction

Given the large numbers of Mediterranean Water eddies or meddies that have been observed in the eastern Atlantic (Armi and Zenk 1984; Richardson et al. 1991) and the long distances they travel (Armi et al. 1989; Richardson et al. 1989), it is likely they play a significant role in producing along-isopycnal fluxes of heat and salt and have an important influence on the large-scale structure of the Mediterranean salt tongue. Roughly 20%–40% of the salt flux out of the Mediterranean is thought to enter the eastern Atlantic in meddies (McWilliams 1985; Richardson et al. 1989). If meddies are important to the heat and salt budgets of the eastern North Atlantic, then it is important to try to understand the mechanisms that make it possible for them to produce these large property fluxes.

In recent years a number of authors have suggested that the motion of meddies can be attributed to the large-scale flows in which they are embedded. Richardson et al. (1989) found that the floats inside meddies moved at roughly 1.4 cm s^{-1}, relative to those floats outside meddies at the same depth (after averaging over the looping motions of the floats), and suggested that meddies were advected by the large-scale flow field above 800 db. More recently, Hogg and Stommel (1990) proposed a simple point–vortex model to explain how a meddy could be advected by currents in the upper thermocline. They suggest that the large-scale vertical shear outside a meddy could interact with the baroclinic structure within the core, causing the meddy to propagate through the surrounding water. When a point–vortex pair is tilted by an external shear, the pair will propagate if the vortices have unequal strengths. The vortex induction mechanism that causes the pair to translate is similar to that discussed by Flierl et al. (1980), who obtained solutions representing barotropic modons with baroclinic "riders."

Walsh (1995) generalized Hogg and Stommel's model to allow for three-dimensional, stratified dynamics and a nonsingular representation of the meddy. The configuration of the idealized meddy used in the model is shown in Fig. 1 [the vertical axis has been stretched to give the lens an $O(1)$ aspect ratio]. The meddy is assumed to be made up of a "core" of anomalously warm and salty water, characterized by low potential vorticity values and strong anticyclonic circulation. Although the T–S signature of the meddy is confined to this core region, the velocity signature predicted by the model extends well beyond the core region. The vertically sheared flow in which the meddy is embedded deforms the meddy core and induces a (time-average) transverse tilt to the core. If the rotation rate within the meddy core varies with depth, this tilt may lead to propagation with respect to the surrounding fluid by a mechanism that is a direct generalization of that discussed by Hogg and Stommel. In Fig. 1 the depth-dependent component of the flow in the core is shown schematically by the oppositely signed "point vortices" near

* Woods Hole Contribution No. 8999.

+ Current affiliation: Department of Oceanography, Dalhousie University, Halifax, Nova Scotia, Canada

Corresponding author address: Dr. David Walsh, Department of Oceanography, Dalhousie University, Halifax, Nova Scotia B3H 4J1, Canada.

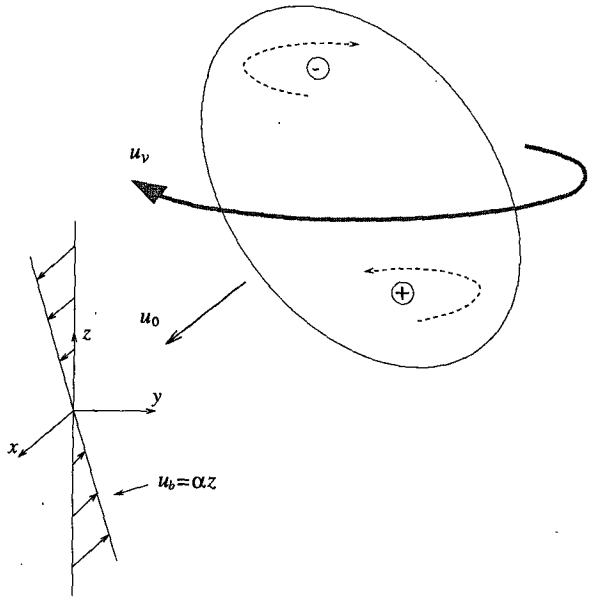

FIG. 1. Sketch of an idealized meddy tilted by background shear. The vertical axis has been stretched for ease of presentation. Vertically sheared external flow in the x direction ($u_b = \alpha z$) induces a (time average) tilt in the y direction. If the rotation rate varies with depth in the core, the tilted meddy can propagate with respect to the surrounding fluid (the differential rotation component is shown schematically by the oppositely signed point vortices near the top and bottom of the meddy core; the strong anticyclonic circulation in and around the core is shown by the shaded arrow labeled u_v). The vertical extent of the meddy is typically 800 m and the radius of the core is on the order of 20 km.

the top and bottom of the meddy, superimposed on the strong anticyclonic flow in the core. If the meddy is transversely tilted by external shear, interactions between the upper and lower "point vortices" will cause the meddy to translate.

In order to search for the lateral tilting of a meddy, we investigated the available SOFAR float data in meddies. We have discovered what we believe to be a tilting of the rotation axes of two different meddies, the only two containing floats at different depths. The observed tilts are attributed to a combination of kinematical and dynamical effects. The tilt of one of the meddies (Meddy 1) is due to the combination of lateral translation and a depth-varying rotation rate. The tilt of Meddy 2 appears to represent a deformation of the meddy core by external flows. In what follows we discuss these observations, and we interpret them using Walsh's (1995) model, which predicts the deformation of a lens induced by a fixed external shear and the resulting translation of the lens. We attempt to relate the propagation of the meddies through the surrounding water to the external shear and the potential vorticity structure within the core using the analytical results discussed by Walsh (1995).

In the following sections we discuss the float data, their analysis, and the results. We then compare these results with model results. Because of the small size of the tilts, float position errors are examined in some detail to verify the results. Finally, we end with the conclusions.

2. Data

The SOFAR float data were obtained as part of an experiment to track meddies in the eastern North Atlantic (Armi et al. 1989; Richardson et al. 1989). Three different meddies were tracked (Fig. 2), two of which contained floats at different depths separated vertically by roughly 100 m (Table 1). The floats looped around the core of Meddy 2 with a period of about 4 days and azimuthal velocities of roughly 30 cm s^{-1} at a radius of 20 km. The flow within the central core region (<20 km) of Meddy 2 was close to solid-body rotation over the range of depths sampled by the floats in the meddy. One float (EB145) in Meddy 3 showed that the rotation frequency was strongly a function of depth beneath the core; the looping period decreased from approximately 23 days to 12 days as the float rose from 1300 db to 1050 db at roughly the same radius (~23 km). The two floats at different depths within Meddy 1 looped with different periods; EB128 at 1121 db looped with a 9-day period, EB150 at 1220 db with a 23-day period (Table 1). Schultz Tokos and Rossby (1991) used current profilers to show that the flow within the core of Meddy 1 was essentially a depth-dependent solid-body rotation.

The SOFAR floats transmitted an 80-sec acoustic signal twice a day at 12-hour intervals. Times of arrival were recorded by three moored Autonomous Listening Stations (ALSs) and were used to calculate float positions by triangulation. The speed of sound used in the calculations, 1.496 km s^{-1}, was chosen by minimizing the difference between the first calculated acoustic fixes and the float launch locations (Price et al. 1986). We estimate that with the tracking configuration used here, the absolute position of a float is determined with an accuracy of a few kilometers. The accuracy in determining the displacement between two nearby floats is considerably better than this, as discussed later. A more complete description of the floats and data is given in two data reports (Price et al. 1986; Zemanovic et al. 1988).

The detailed structure of the flow field outside the meddies is unknown. Perhaps the most detailed information about the mean shear in the Canary Basin can be found in the study by Saunders (1981), who computed geostrophic velocity profiles from several sections in the eastern North Atlantic. The two southernmost sections, one at 32°N and another extending from 30°N, 25°W to 38°N, 17°W, show that the flow is generally southward with larger velocities near the surface. An increase in the flow speed of about 0.3 cm s^{-1} between 1500 db and 500 db occurs in the 32°N section; a much larger variation of almost 2 cm s^{-1} over the same range of pressures is seen in the second section.

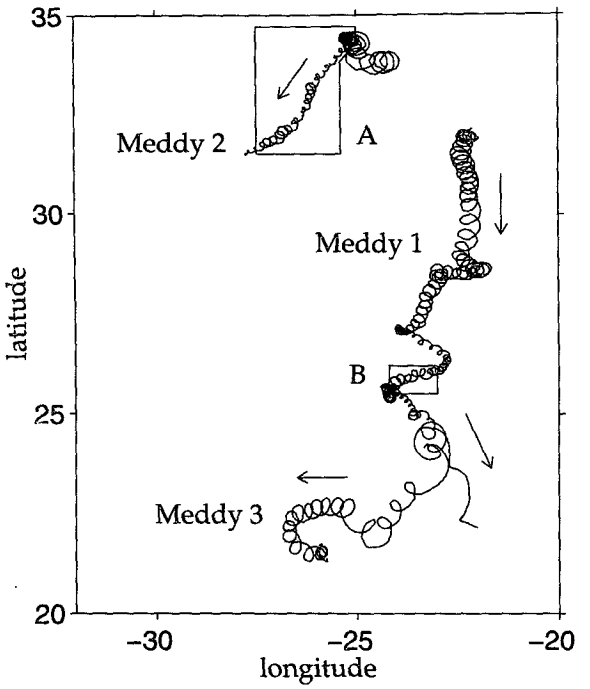

FIG. 2a. Translation of three different meddies as given by the trajectories of SOFAR floats: EB128 in Meddy 1 between Oct 1984 and Oct 1986, EB148 in Meddy 2 (Nov 1985–Jul 1986), and EB145 in Meddy 3 (Sep 1985–Mar 1987) (adapted from Richardson et al. 1989). Two floats at different depths were located in both Meddies 1 and 2. The portions of meddy trajectories discussed in the paper are shown by the boxes labeled A (Meddy 2) and B (Meddy 1).

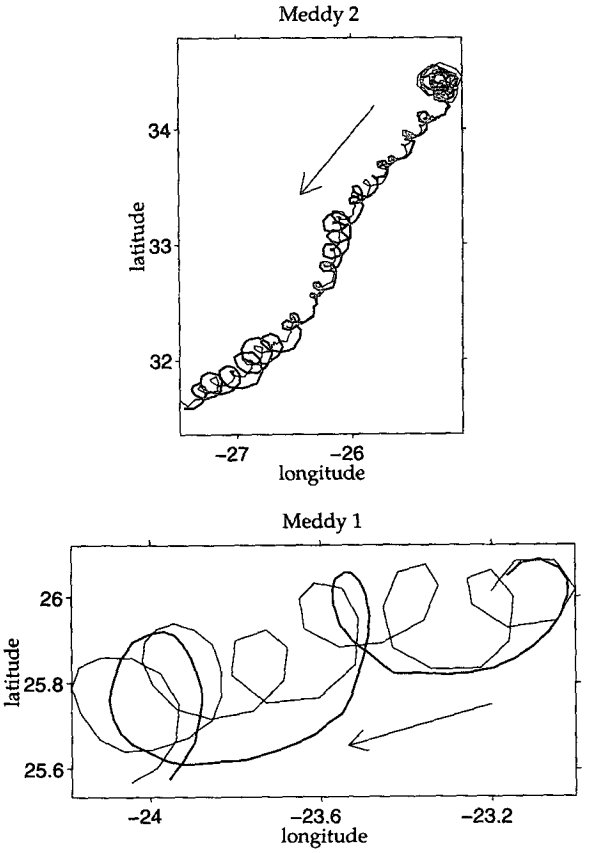

FIG. 2b. Enlarged view of the portions of the trajectories used in the analysis (corresponding to the boxes A and B in Fig. 2a), showing pairs of float trajectories at different depths in the two meddies used in our analysis. The upper plot shows the trajectories of floats EB149 (thin line) and EB148 (thick line) between 14 Feb and 29 Jun 1986. The lower plot shows the path of floats EB128 (thin) and EB150 (thick) between 4 Jan and 5 Mar 1986. These portions of the meddy trajectories were chosen for the analysis because they were the steadiest in speed and direction. Only a relatively short section of the overall trajectory of Meddy 1 contained floats at two different depths.

At 32°N there is virtually no meridional flow at 1000 db near the core of the salt tongue, consistent with the low mean velocity from floats outside meddies. Since we do not have real-time information about the background shear outside of the meddies, we will assume that the direction of meddy translation is a proxy for the shear. If the meddy drift velocity is a weighted average of the external velocity field over the meddy core, then the direction of the external shear is well represented by the drift vector, if not the actual absolute magnitude of the shear.

3. Data analysis

To investigate the tilt of the rotation axis of the meddies, it was necessary to calculate the center of rotation from float trajectories at different depths in the meddies. A low-pass filter was used to remove the looping component from the float trajectories and to give an estimate of the position of the meddy center as a function of time. This technique worked quite well, probably because of the large spectral gap between the looping motions of the floats and the motions of the meddy as a whole. However, it failed when the trajectory of the meddy turned sharply or when the looping frequency of the float changed suddenly. In the present analysis only two well-behaved sections of the trajectories were used (Fig. 2). By well behaved, we mean that the direction and speed of the meddy were fairly steady. Due to the different looping frequencies of the floats, it was necessary to use several different filters in the analysis. For float EB150 a 61-day moving-average filter having Gaussian filter weights with a standard deviation of 11 days was used, providing a frequency response of 0.5 at a frequency of about $1/55$ cycles day^{-1}, with higher frequencies being more strongly attenuated. For EB128 a 31-day filter with a standard deviation of 5.7 days was used, giving a frequency response of 0.5 at $1/28$ cycles day^{-1}. For floats EB148 and EB149, a filter with a standard deviation of 4.0 days was used, giving a frequency response of 0.5 at $1/20$ cycles day^{-1}.

An alternative way also used to compute the drift speeds, rotation frequencies, and looping radii [used by

TABLE 1. Summary of meddy float data. Values are averages over the listed period of time.

	Meddy 2		Meddy 1	
Dates studied	14 Feb–29 Jun 1986		4 Jan–5 Mar 1986	
Duration	135 d		60 d	
Translation speed (cm s^{-1})	3.1		1.9	
Translation direction (° True)	207		240	
Float IDs	EB148	EB149	EB128	EB150
Transmit time[a] (UTC)	0940	1000	0120	1020
Pressure (dbar)	1129	1024	1121	1220[b]
Temperature °C	>12.0[c]	12.6	10.0	8.2
Period of loops (days)	4	4	9	23
Radius of loops (km)	8.4	6.2	12.6	16.3
Number of loops	33	33	7	2.5
Swirl velocity (cm/sec)	13.6	10.4	9.5	4.8

[a] The floats transmitted two signals per day, 12 hours apart. The listed time is the first transmit time of the day.

[b] The pressure record indicated that EB150 was below 1200 db, the deepest observable pressure. The mean temperature of 8.2°C measured by this float combined with a temperature section through Meddy 1 in Oct 1985 (Hebert 1988) suggests that the float was at roughly 1220 db. The maximum temperature in the well-mixed core of the meddy in Oct 1985 was around 12°C at 900 m, indicating that both floats EB128 and EB150 were beneath the core of the meddy.

[c] EB148 measured ~11.9°C just before this period of time, but during this period the float thermometer was pegged at 12.0°C (the maximum observable temperature), indicating temperatures warmer than 12°C. During the time of the tilt study, both floats EB148 and EB149 rose by approximately 40 m in the core of Meddy 2.

Armi et al. (1989)] was to divide the time series of positions into a number of shorter sections, fitting each section to a model of the form

$$X_n(t) = X_{n0} + U_n t + R_n \cos(\omega_n t + \phi_n)$$
$$Y_n(t) = Y_{n0} + V_n t + R_n \sin(\omega_n t + \phi_n), \quad (1)$$

where the subscript n refers to the nth section. Thus, each section of a trajectory was decomposed into a linear drift plus a circular looping component. The model parameters were fitted using standard nonlinear least-squares algorithms as given by Press et al. (1986), which gave satisfactory results when the initial guesses were reasonably good. The technique seemed to give results inferior to those of the low-pass filtering,[1] so we have used the results of the filtering technique exclusively in this work. However, the good overall agreement between the two methods indicates that the filtering results are quite robust.

[1] The inferior results are probably due to the fact that the parameters U_n and V_n are derivatives of the original position time series, which tends to amplify any errors in the calculation.

4. Results

To illustrate the tilt of the meddies with respect to their translation direction, we plotted a time series consisting of a displacement vector connecting the centers of rotation for float pairs (showing the "tilt") superimposed on a meddy drift velocity vector for the same time (Fig. 3). The most notable feature in Fig. 3 is the tendency of the meddy rotation axes to tilt in a direction perpendicular to their drift direction. Meddy 2 appears to be in this configuration for most of the 135 days shown: maximum displacements are almost one kilometer in mid-June 1986.

Meddy 1 displacements are much larger than those of Meddy 2, sometimes approaching 10 km, although the translation of Meddy 1 is somewhat slower than Meddy 2. The general pattern is the same, however, with displacements normal to the meddy drift direction. The average displacement measured for Meddy 2 was 0.41 km and the mean drift speed was 3.1 cm s^{-1}; the average displacement measured for Meddy 1 was 6.5 km and its average drift speed was 1.9 cm s^{-1}. Note that the upper part of both meddies is deflected to the right (northwest) with respect to their translation directions (southwestward). Because both floats in Meddy 1 were below the well-mixed core, we interpret the displacements as representing the distortion of the external trapped fluid region that is carried along with the translating meddy.

A summary of the information given in Fig. 3 is shown in Fig. 4a. Each symbol represents the tip of a vector, the length of which measures the ratio of the meddy drift speed to the horizontal displacement of the rotation axis. The angle between the vector and the horizontal axis represents the angle between the velocity vector and the displacement vector. Absolute displacements $\sqrt{\Delta x^2 + \Delta y^2}$ of less that 0.2 km are not shown, as we believe that the data are not sufficient to resolve such small displacements. Velocities less than 3.0 cm s^{-1} are shown by small circles; larger velocities are shown by crosses. Notice how the points tend to cluster along the vertical axis, especially for drift speeds less than 3.0 cm s^{-1}. This illustrates the tendency for the rotation axis to tilt at right angles to the drift direction of the meddy. The average deflection angle for Meddy 1 is 84°, while for Meddy 2 it is 111°. If the directions were random, we would expect that approximately 17% of the vectors would fall into the 60° sector bracketing the vertical axis. Most (95%) of Meddy 1 vectors fall into this sector, clearly illustrating the systematic tilt. A somewhat smaller percentage (62%) of the data from Meddy 2 fall into this sector, although 95% of the data with speeds less than 3.0 cm s^{-1} lies within this range.

Plotting the data in a slightly different way reveals an apparent relationship between the tilt of the rotation axis and the translation speed of the meddy. In Fig. 4b the zonal (u) velocity component of the meddy drift

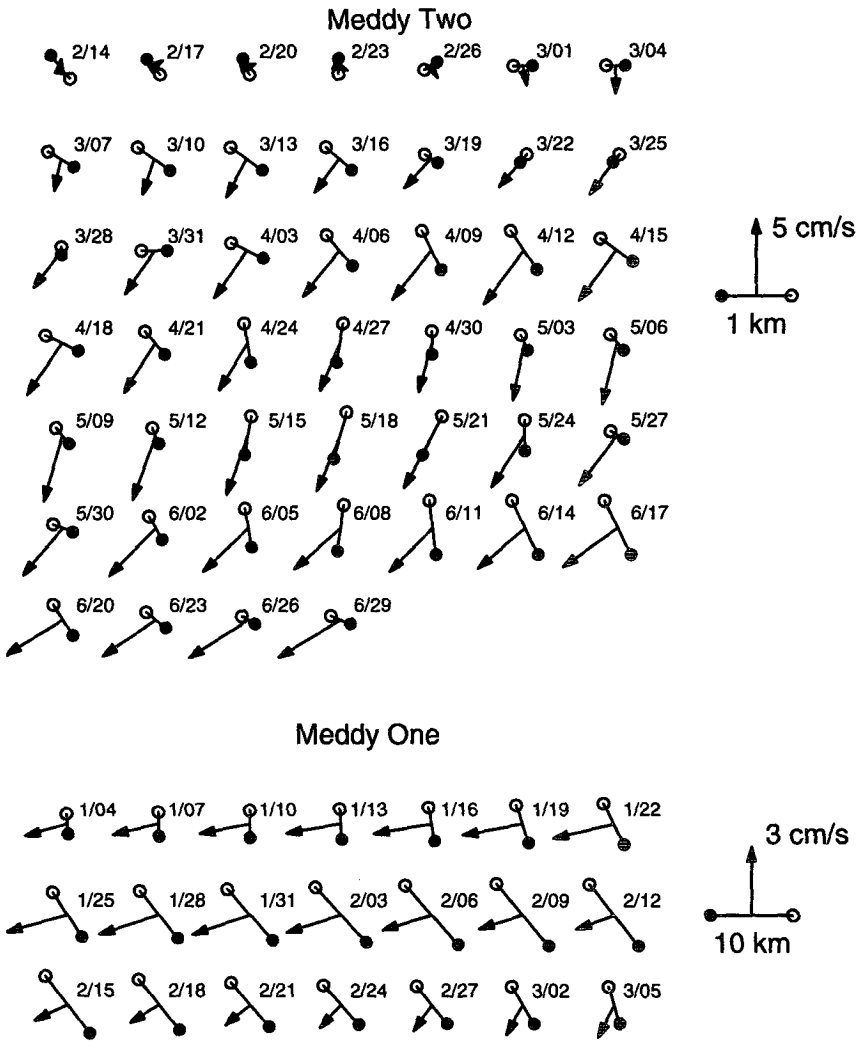

FIG. 3. Realizations of meddy drift velocity (represented by arrows), and tilt for two different meddies, shown by plotting the center of rotation at two different depths. Circles (○) show the rotation axis calculated from the trajectory of the shallower float; filled circles (●) show the rotation axis of the deeper float. (a) Meddy 2 during the period from 14 Feb 1986 through 29 Jun 1986. (b) Meddy 1 from 4 Jan 1986 to 5 Mar 1986. Notice that both meddies are generally tilted in a direction perpendicular to their drift direction, with the shallower float on average northwestward of the deeper float.

speed is plotted against the y displacement of the rotation axis (shown by small circles), and the meridional velocity (v) is plotted versus the negative of the x separation (shown by crosses). As in Fig. 4a, absolute displacements less than 0.2 km are not shown. The top panel (I) shows all data for Meddy 2; panel (II) shows all Meddy 2 data with drift speeds less than 3.0 cm s^{-1}; panel (III) shows all Meddy 1 data. Comparing panels (I) and (II) shows that there is apparently a strong correlation between the translation speed of Meddy 2 and the displacement of the rotation axis for speeds less than 3.0 cm s^{-1}, but that this simple relationship breaks down for unknown reasons when the drift speed of the meddy exceeds 3.0 cm s^{-1}. The data for Meddy 1 (panel III) show a similar trend, with larger displacements associated with larger speeds, although low-frequency fluctuations about this trend also occur. A linear relationship between drift speed and tilt is in agreement with the model discussed by Walsh (1995).

5. Model comparison

The observed transverse tilt of the meddies can be understood using the analytical model of a quasigeostrophic lens in a stratified fluid discussed by Walsh (1992, 1995). When the lens (initially assumed to be

axisymmetric) is perturbed, the induced boundary perturbation will propagate in a wavelike fashion around the lens. To demonstrate this, consider the behavior of a small boundary perturbation imposed on an initially circular two-dimensional eddy with uniform negative

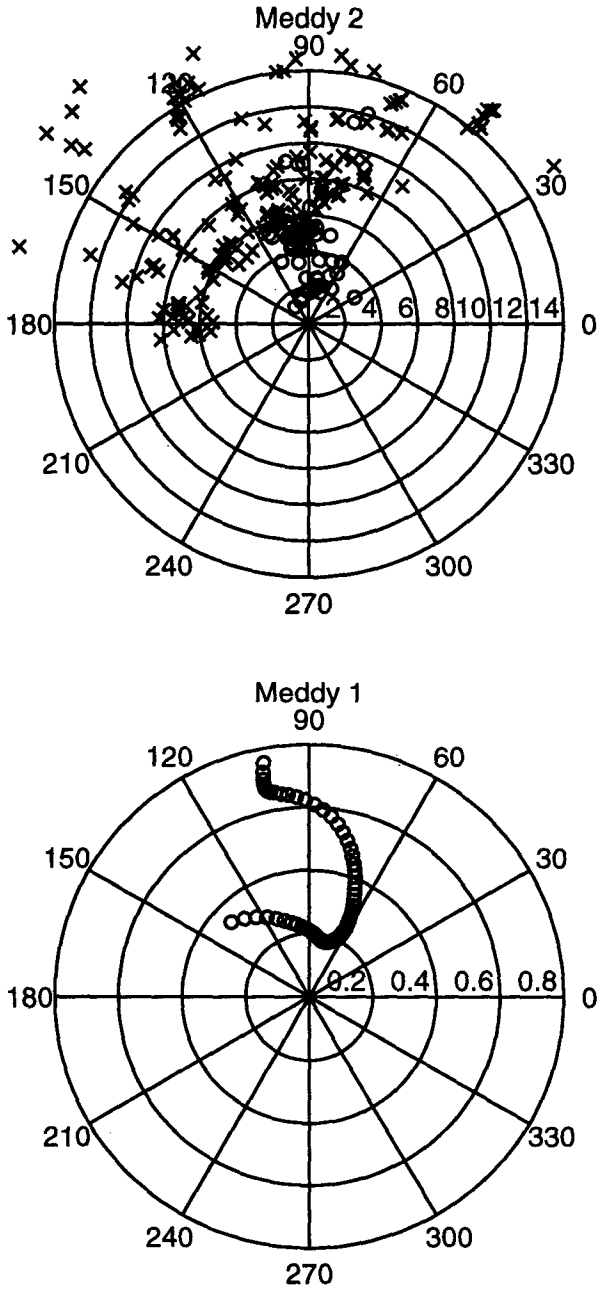

FIG. 4a. Statistical summary of meddy velocity and tilt data. Daily realizations of the meddy configuration are represented by vectors of length l and angle Θ, where l (cm s^{-1} km^{-1}) is the ratio of the drift speed to the horizontal displacement of the rotation axis and Θ (degrees) is the angle between the displacement vector and the velocity vector. The circles (○) and crosses (×) represent the tips of these vectors. Velocities larger than 3 cm s^{-1} are shown by crosses.

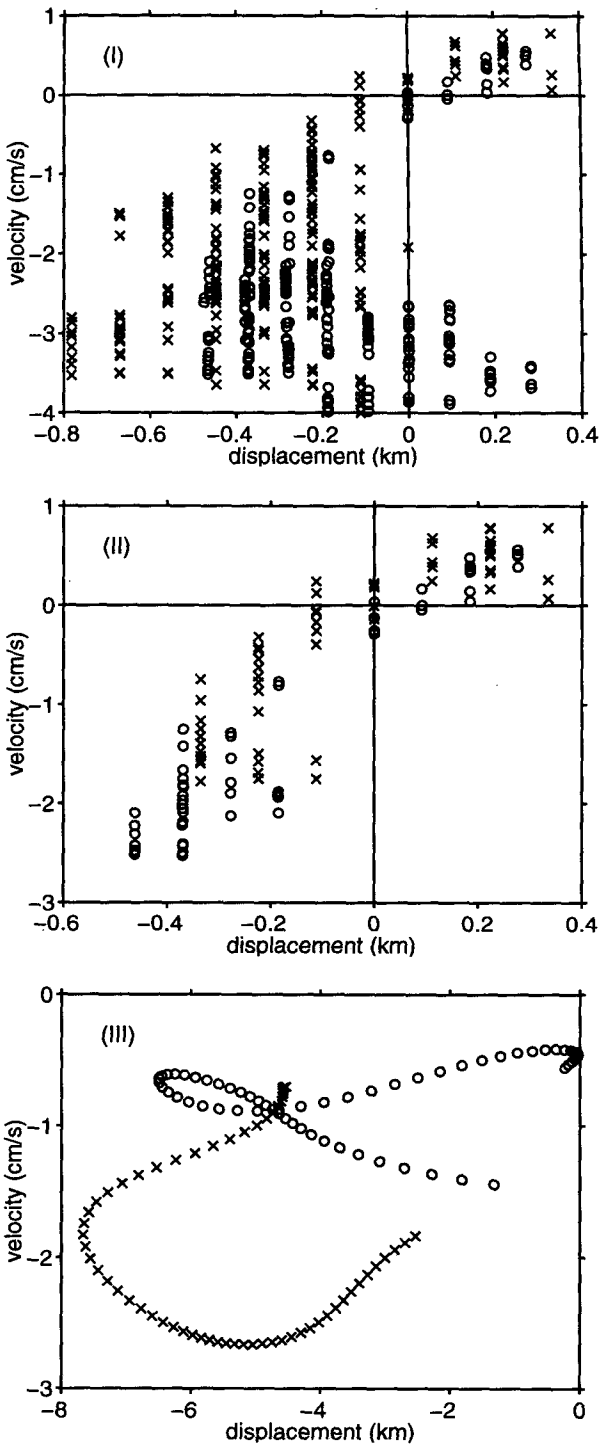

FIG. 4b. The x displacement of the rotation axis is plotted against the v velocity component (circles), and the *negative* of the y displacement versus the u velocity component (crosses). Panel I shows all data (daily values) for Meddy 2, panel II shows Meddy 2 data with velocities less than 3 cm s^{-1}, and panel III shows the data for Meddy 1. The data indicate that there is a fair correlation between the amount of deflection of the rotation axis and the speed of Meddy 2 when the meddy is translating at less than 3 cm s^{-1}.

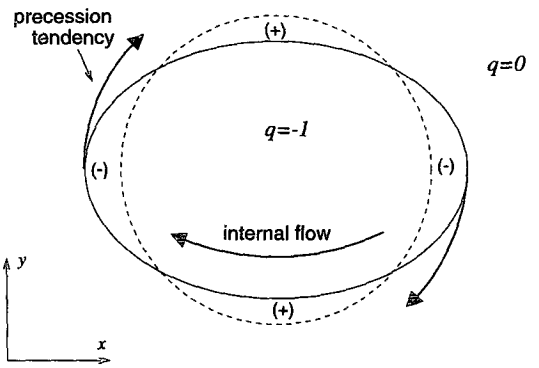

FIG. 5. Illustration of the mechanism by which boundary perturbations can propagate, causing precession of the core. The combination of the basic-state anticyclonic flow and the small potential vorticity (q) anomalies [denoted by (+) and (−)] associated with the boundary deformation cause the deformed eddy to precess in an anticyclonic sense.

potential vorticity (Fig. 5). The potential vorticity anomalies induced by the boundary deformation propagate in a cyclonic sense relative to the fluid. However, the strong anticyclonic flow inside the core generally overwhelms this propagation tendency, resulting in an anticyclonic precession of the core. When an external shear is present, steady configurations are possible in which the tendency of the eddy to precess is counterbalanced by external shear. These ideas translate directly to the three-dimensional case, and a possible steady configuration for a three-dimensional lens is illustrated in Fig. 1. In this figure the lens is tilted in a transverse sense by vertically sheared external flow. Walsh showed that the magnitude of the equilibrium boundary deformation is directly proportional to the strength of the external vertical shear and varies inversely with the intensity of the flow within the lens.

Walsh considered the behavior of a lens-shaped eddy in an unbounded, uniformly stratified fluid with uniform external shear. The analytical model he used is based on the premise that the flow is approximately geostrophic, that the external shear is "weak," and that the eddy is sufficiently small and intense that variations of the Coriolis parameter f_0 with latitude can be neglected. Beginning with these assumptions, he employed a linearized "contour dynamics" approach to investigate the behavior of a lens deformed by external shear. Because these linearized results require that the deformation of the meddy core induced by the external flow is small (i.e., the shear is weak), and that the flow is quasigeostrophic (QG), we must check whether these assumptions are justified before comparing the model predictions with meddy observations. The Rossby number for Meddy 2 is

$$\mathrm{Ro} = \frac{U_{\max}}{f_0 R} \approx 0.23,$$

which is small enough to justify quasigeostrophy as a first-order approximation. Next, the deflections shown in Fig. 4a are much smaller than the meddy radius, so the behavior of Meddy 2 should be adequately represented by these linear calculations. While we have no direct measure of the distortion of the core of Meddy 1 (since both floats were beneath the core), its Rossby number is estimated to be ~0.18, so it seems reasonable that the theoretical results will be applicable.

The analytical model is expressed in terms of the dimensionless variables

$$(x, y) = (x_*, y_*)/R$$

$$z = z_*/D(ND/f_0R)$$

$$r = \sqrt{x^2 + y^2 + z^2}$$

$$\alpha = \frac{\partial u_{b*}/\partial z_*}{|\bar{q}_*|}\frac{D}{R}\left(\frac{f_0R}{ND}\right) = \frac{\partial u_{b*}/\partial z_*}{|3U_{\max}|}D\left(\frac{f_0R}{ND}\right)$$

$$b = \frac{\partial q_{v*}/\partial z_*}{\bar{q}_{v*}}D, \qquad (2)$$

where an asterisk denotes a dimensional quantity, D is equal to *half* the thickness of the lens, R is its radius, and distances are measured relative to a coordinate frame located at the center of the meddy. The parameter α measures the strength of the external vertical shear, and b is a measure of the differential rotation within the meddy core. The dimensionless quasigeostrophic potential vorticity is taken to be of the form

$$q = \begin{cases} -1 - bz \equiv q_v, & r < 1 \\ 0, & r > 1. \end{cases} \qquad (3)$$

If $b = 0$, the potential vorticity within the core ($r < 1$) is constant and the core region will be in solid-body rotation; if b is nonzero, the rotation frequency within the core varies with depth. For the moment we will assume that $b = 0$, as this simplifies the calculation considerably, yet still permits an investigation of the tilting induced by external shear. The model formulation assumes that the Burger number $(ND/f_0R)^2 = 1$; that is, the radius R is equal to one deformation radius. In this case, an eddy with a small aspect ratio in physical space will have unit aspect ratio in the scaled coordinate system defined by (2a,b); our analysis will focus on eddies that are approximately spherical in these transformed coordinates. Lastly, we take the external flow field to be a uniform vertical shear:

$$u_b = \alpha z, \qquad (4)$$

where the depth-averaged external velocity is taken to be zero to remove the effect of a bulk advection of the meddy by external currents. The idealized model eddy is sketched in Fig. 6.

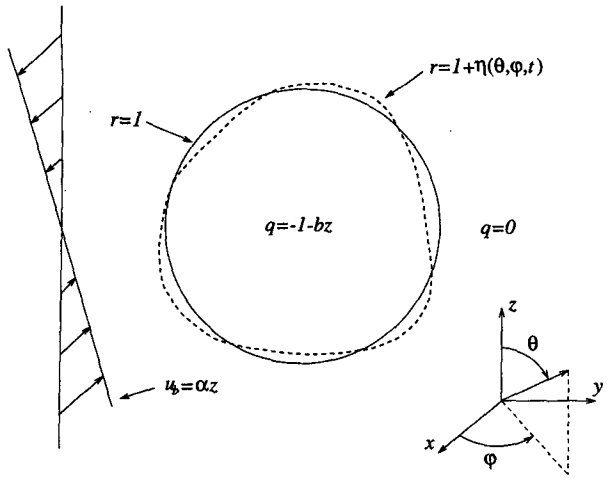

FIG. 6. Sketch of a continuously stratified, three-dimensional eddy characterized by anomalous quasigeostrophic potential vorticity (q), illustrating the physical premise for the analytical model discussed in the text. The eddy is embedded in "weak" external shear, and is deformed due to interactions with the external flow.

a. Meddy deformation

The boundary of the core region is given by $r = 1 + \eta$, and the predicted equilibrium boundary deformation is given by

$$\eta_F = -\frac{15}{4}\alpha \sin 2\theta \sin\varphi, \tag{5}$$

where θ is the polar angle and φ the azimuth angle (see Fig. 6). In dimensional terms this gives an amplitude of

$$|\eta_*| = \frac{5}{4}\left|\frac{\alpha_* D}{U_{\max}}\right| R. \tag{6}$$

If we take $D = 400$ m, $R = 20$ km, $U_{\max} = 30$ cm s^{-1} as representative values for Meddy 2 and if we assume that $\alpha_* \equiv \partial u_{b*}/\partial z_* = 2.5 \times 10^{-5}$ s^{-1}, corresponding to a variation in the external flow speed of 2 cm s^{-1} over the core depth, we find that

$$|\eta_*| \approx 0.8 \text{ km}. \tag{7}$$

The maximum horizontal deformation of the meddy should then be twice this value, or about 1.6 km. This is somewhat larger than the results in Fig. 3a would indicate, because the floats are quite close together in the vertical, so the full extent of the tilting is not seen. If the maximum boundary deformation occurs over a depth range of about half the thickness of the lens (~400 m) then the observed displacements shown in Fig. 4a should be about 1/4 of the total predicted boundary deformation, since the floats are about 100 m apart in depth. Thus, the displacements shown in the figure are in good agreement with the model prediction of $1/4 \times 1.6$ km $= 0.4$ km.

Because the velocity field of the meddy can be derived from the float data, while the core-deformation discussed in the previous paragraph cannot, it will be useful to consider the flow field associated with the deformed eddy. It can be shown (Walsh 1992, 1995) that the total flow field for the equilibrium solution (5) (again for the case in which $b = 0$) is given by

$$\mathbf{u}_*(r,\theta) = \underbrace{-U_{\max} r \sin\theta \begin{pmatrix} 1 \\ 1/r^3 \end{pmatrix} \hat{\varphi}}_{\text{I}} + \underbrace{3U_{\max}\alpha z \mathbf{x}}_{\text{II}}$$

$$+ \underbrace{\frac{9}{2} U_{\max}\alpha z \begin{Bmatrix} \mathbf{x} \\ r^{-5}(1 - 5y^2/r^2)\mathbf{x} + 5xyr^{-7}\mathbf{y} \end{Bmatrix}}_{\text{III}}, \quad \begin{matrix} r < 1 \\ r > 1 \end{matrix} \tag{8}$$

where $\mathbf{x}$, $\mathbf{y}$, $\mathbf{z}$, and $\hat{\varphi}$ are unit vectors, and $U_{\max}$ ($\equiv |\bar{q}_{v*}| R/3$) is the maximum azimuthal velocity at the edge of the meddy core. The terms labeled I are due to the basic-state (unperturbed) spherical eddy, II is the imposed background flow, and III represents the (equilibrium) dynamical response of the eddy. By dynamical response, we refer to the secondary pressure and velocity fields associated with the deformation of the meddy. The basic-state flow field (I) is in solid-body rotation within the core ($r < 1$), with speeds decreasing monotonically outside the core ($r > 1$). The total flow within the core is a superposition of a solid-body rotation (term I) and a uniform vertical shear in the x direction (terms II and III). Notice that the magnitude of this vertically sheared flow is significantly larger (by a factor of $2\frac{1}{2}$) than the background vertical shear, so the deformation of the meddy has the effect of *increasing* the vertical shear within the core.

To find the slope of the rotation axis inside the meddy core, we set the u velocity component in (8) equal to zero, giving

$$\frac{y}{z} = \frac{15}{2}\alpha = \frac{5}{2}\frac{\alpha_* D}{U_{\max}}, \tag{9}$$

where the slope is measured relative to the z axis. If the dynamical response of the meddy is neglected (i.e., if we simply superimpose the background flow on the basic-state meddy flow field), then the predicted axis slope is

$$\frac{y}{z} = 3\alpha = \frac{\alpha_* D}{U_{\max}}, \tag{10}$$

where $\alpha_* \equiv \partial u_{b*}/\partial z_*$ measures the background vertical shear. Notice that (10) predicts a slope $2\frac{1}{2}$ times smaller than (9), so the flow associated with the dynamical response of the meddy should make an important contribution to the observed tilt in the core. Fig-

ure 7 shows the flow field predicted by (8). Figure 7a shows the flow field of the undeformed meddy in the absence of external flow (term I) for the case in which $b = 0$ and $U_{max} = 22$ cm s^{-1}. Figure 7b shows the superposition of the meddy flow with the background flow (terms I + II) with $\alpha = 0.02$ (corresponding to a variation in u_{b*} of 2.6 cm s^{-1} over the depth of the core). Figure 7c shows the total flow field predicted by linear theory, including the dynamical response of the meddy (terms I + II + III). The parameters used in Fig. 7 are chosen to be roughly appropriate for Meddy 1. Notice that the "kinematic" tilting within the core shown in Fig. 7b is considerably smaller than the total tilt that would actually be measured by two floats in the core (Fig. 7c). Notice also that the rotation axis beneath the meddy core is very distorted, and is not significantly affected by allowing for the dynamical response of the meddy.[2] Thus, if both floats are beneath the meddy core we would expect the dynamical response of the meddy to make little contribution to the total observed tilt.

The total displacement of the rotation axis over the core depth, according to (9), is

$$\Delta y_* = \frac{5\alpha_* D}{U_{max}} R. \tag{11}$$

Using the parameter values previously estimated for Meddy 2 ($D = 400$ m, $R = 20$ km, $U_{max} = 30$ cm s^{-1}, $\alpha_* \equiv \partial u_{b*}/\partial z_* = 2.5 \times 10^{-5}$ s^{-1}), it follows that $\Delta y_* \approx 3$ km. Because the floats were separated by about 1/8 of the core thickness, the predicted axis displacement over the depth range sampled by the floats is $\Delta y_* \approx 3$ km/8 ≈ 0.4 km, which is in excellent agreement with the displacements shown in Fig. 3a.

If the dynamical response is neglected, then (9) and (10) imply that the tilt will be 2 1/2 times smaller than that given by (11). The predicted kinematic displacement for two floats separated by ~100 m in the core is then $\Delta y_* \approx 0.16$ km. This predicted kinematic displacement is significantly less than the displacements shown in Fig. 3, so we conclude that the floats are, in fact, measuring a deformation of the meddy core induced by the background flow.

To estimate the displacements predicted by the model for Meddy 1 (where both floats were apparently beneath the core), we require an expression describing the distortion of the rotation axis outside the meddy core. Because Fig. 6 indicates that the tilt beneath the core is not significantly changed by allowing for the dynamical response of the meddy, we can estimate this using a simple kinematic argument. The argument is based on the idea that the Lagrangian center of an eddy is displaced from the Eulerian center if the eddy is in motion (e.g., Flierl 1981). If the radian frequency at the depth of the shallower float is given by ω_S, the external flow speed at this depth by $\bar{u}_S$, and the meddy translates with speed u_0, then the rotation axis of the meddy will be shifted by an amount

$$\delta_S = (\bar{u}_S - u_0)/\omega_S \tag{12}$$

relative to the position it would have if there were no externally imposed flow and the meddy were not translating. This formula assumes that the flow field within the meddy is a depth-dependent solid-body rotation, as reported by Richardson et al. (1989) and Schultz Tokos and Rossby (1991). The shift of the eddy center at the depth of the shallower float relative to that at the depth of the deeper float is then given by

$$\Delta \equiv (\delta_S - \delta_D) = (\bar{u}_S - u_0)/\omega_S - (\bar{u}_D - u_0)/\omega_D. \tag{13}$$

For Meddy 1 the rotation frequency of the shallower float is more than two times that of the deeper float, and we can expect this differential rotation to make an important contribution to the observed tilt. If the meddy translation velocity u_0 is 1.9 cm s^{-1} and the rotation frequencies of the shallower and deeper floats are 1 cycle/9 days ($\omega_S = -8.1 \times 10^{-6}$ s^{-1}) and 1 cycle/23 days ($\omega_D = -3.2 \times 10^{-6}$ s^{-1}), respectively, and if we take $\bar{u}_S = \bar{u}_D \approx -1.0$ cm s^{-1}, then (13) predicts a displacement of about 5.5 km in the same sense as that shown in Fig. 3b. Allowing for a background vertical shear of 0.25 cm s^{-1}/100 m (equivalent to the value $\alpha_* = 2.5 \times 10^{-5}$ s^{-1} used in the calculation for Meddy 2) increases the predicted tilt by just 14%, so the displacements observed in Meddy 1 can be almost entirely accounted for by this "Lagrangian" tilting mechanism. It follows that the observed displacements for Meddy 1 do not indicate an actual deformation of the meddy core, but are instead due to a superposition of the meddy drift velocity and the depth-dependent circulation beneath the core. This interpretation is consistent with the pressure and temperature data, which indicate that these floats (EB128 and EB150) were beneath the core of the meddy.

According to the preceding discussion, the observed tilts can be divided into three categories: 1) tilting of the rotation axis by superposition of an external shear ("shear" tilting), 2) tilt caused by the translation of an eddy with vertically varying rotation rate ("Lagrangian" tilting), and 3) tilting associated with an actual deformation of the eddy core by external flows ("dynamical" tilting). The first two are inherently kinematic, as they do not account for the response of the eddy to the external shear or translation; the third is dynamical in nature, and results from the secondary flow associated with the deformation of the meddy core. For Meddy 1 the observed tilt can be almost entirely accounted for by the Lagrangian tilting mecha-

[2] This is because the flow associated with the dynamical response decays as r^{-4} outside the core, compared with r^{-2} for the basic-state meddy flow field.

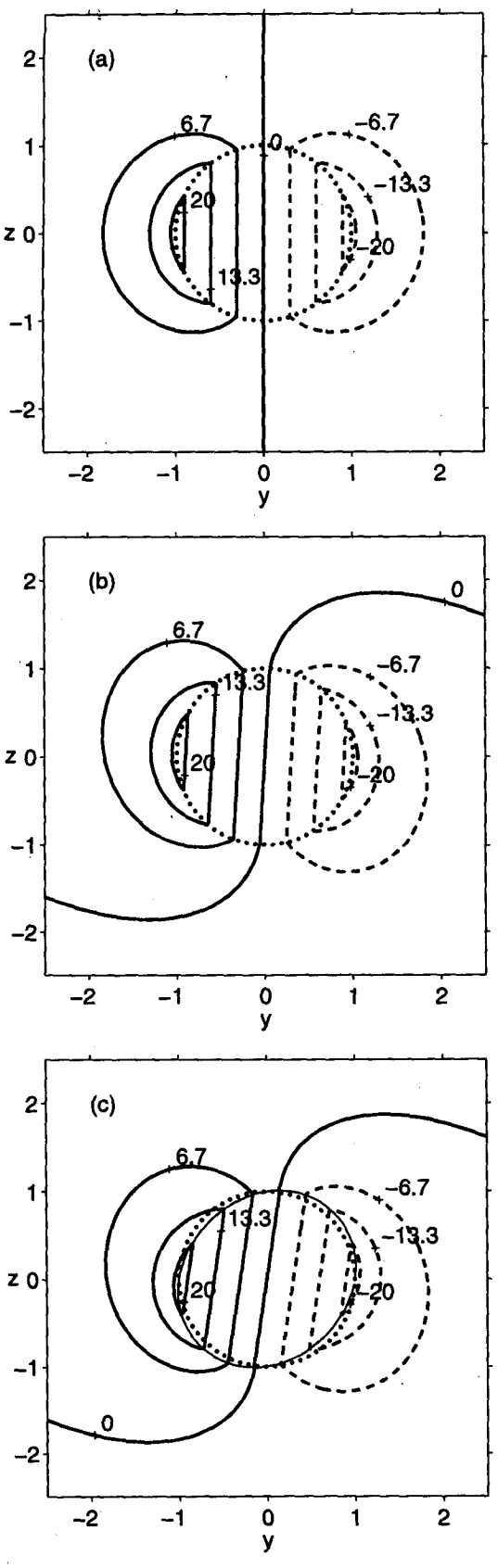

nism, while for Meddy 2 the observed tilts are accounted for by a combination of kinematic "shear" tilting, and an additional tilt associated with the dynamical response of the meddy to the imposed shear. These results are summarized in Table 2.

Although the discussion in this section has tacitly assumed that the lens is in equilibrium with the external forcing, there is no obvious reason why the lens should be in equilibrium, since the external conditions are constantly changing. A quasi-equilibrium behavior is possible when the period of the normal-mode boundary deformation forced by the external flow is much smaller than the timescale on which external conditions vary, so that the lens can quickly re-equilibrate when external conditions change. However, one can also envisage a situation in which the solution is periodic in external shear. In such cases the boundary perturbation can be considered to have two components, one in steady equilibrium with the external shear (the forced component) and another which precesses freely. This would lead to a periodic modulation of the boundary with a period given by the precession period of the free mode, although the lens should still have a time-average transverse tilt similar to what is observed. Using Eq. (25) from Walsh (1995) it can be shown that a normal-mode boundary perturbation will precess anticyclonically with a precession period P given by

$$P = \frac{2\pi R}{U_{\max}[1 - 3/(2n + 1)]} = \frac{\text{Meddy rotation period}}{1 - 3/(2n + 1)}, \qquad (14)$$

where the wavenumber n controls the vertical structure of the boundary perturbation. The deformation shown in Fig. 1 represents an $n = 2$ [see Walsh (1995) for details], so the precession period for this mode should be $2\frac{1}{2}$ times larger than the rotation period of the core. For Meddy 2 (which had a rotation period of four days) this predicts a precession period of 10 days. It is likely that any freely precessing component of the response is partially filtered out in our analysis, causing the response to look steadier than it really is. Nevertheless, it seems probable that some of the "scatter" seen in Fig. 4 is caused by precession of the core.

FIG. 7. Illustration of the different factors contributing to meddy tilt. Panel (a) contours a cross section (in the $y - z$ plane) of the u-velocity field for the basic-state eddy (for the case $b = 0$, $U_{max} = 22$ cm s^{-1}). (b) A uniform external vertical shear in the x direction ($\alpha = 0.02$) is superimposed on the basic-state flow field. (c) The flow resulting from the distortion of the meddy core (the "dynamical response") is added. The dotted curves show the shape of the unperturbed eddy; the thin solid line in (c) shows the equilibrium shape of an eddy deformed by external shear. The dynamical response of the meddy causes the rotation axis to tilt more than would be expected from simple kinematic arguments.

TABLE 2. Summary of observed and predicted axis displacements over an ~100 m depth interval. "Kinematic" displacements result from the superposition of the flow field of a translating meddy and a uniform external shear. The total predicted displacement includes both the kinematic displacement and that resulting from the dynamical response of the meddy.

	Meddy 2	Meddy 1
Mean observed displacement (km)	6.5	0.41
Predicted "kinematic" displacement (km)	5.5	0.16
Total predicted displacement (km)	~5.5	0.4

b. Meddy translation

Walsh derived an integral expression [Walsh 1995, Eq. (32)] showing that a quasigeostrophic lens with depth-dependent core potential vorticity in a vertically sheared flow translates at a rate that is different than the mean external flow speed advecting the core. This result does not rely on assumptions about the functional form of the external flow field u_b, the core potential vorticity q_v, or about the size or constancy of the Burger number ND/f_0R, and hence is quite general. For the special case illustrated in Fig. 6 (i.e., constant external vertical shear, $(ND/f_0R) = 1$, and $q_v = -1 - bz$), the predicted propagation speed relative to the external fluid is

$$u_{0*} = -\frac{1}{5}\alpha_* Db. \tag{15}$$

Thus, the translation speed is completely determined when the potential vorticity within the lens and the magnitude of the external vertical shear α_* are specified. The propagation mechanism is analogous to that considered by Hogg and Stommel (1990), who found that a baroclinic point vortex pair tilted by external shear will propagate through the surrounding water. Walsh (1995) showed that the predicted propagation is equivalent to an advection of the "center of potential vorticity" of a lens by the external flow, and the translation speed is given by a potential vorticity weighted average of the external velocity over the core region. If we can assume that the meddy potential vorticity field is one-signed, then this implies that the meddy translation speed *must* lie within the range of external flow speeds seen over the core region. Assuming a vertical variation in external flow speed of 2 cm s^{-1} over the depth of the core, it follows that the *maximum* possible propagation speed for the meddy (relative to the average external flow velocity over the core region) is 1 cm s^{-1}.

To make more precise predictions of the translation velocity we must estimate the value of the parameter b in (15), which is a measure of the vertical variation of the rotation rate within the core. In principle this may be done by measuring the vertical variation of the rotation rate within the core, and choosing b to reproduce this in the model velocity field. Unfortunately, this is difficult to do using our float data, since for Meddy 1 neither of the two floats was in the meddy core, while for Meddy 2 both floats were in the core, but they were separated by only ~100 m in the vertical, so the core was not well sampled in depth. Theory can provide some guidance, however, as Walsh (1995) has found that solutions representing a baroclinic lens in shear exist only when $|b| \leq 5/3$, which allows an upper bound to be placed on the value of b. Furthermore, recent observational studies show that in some cases there may be large variations in rotation rate within the core of a meddy. For example, Prater and Sanford (1994) documented a meddy off Cape St. Vincent that comprised "two distinct, vertically aligned lenses." The upper lens was characterized by maximum velocities of 23 cm s^{-1}, while the lower lens was much less intense, with peak azimuthal velocities of about 12 cm s^{-1}. According to the discussion in the previous paragraph, we would expect the translation speed of such a meddy to be close to that of the external flow at the depth of the more intense "upper core."

While the observations discussed by Prater and Sanford (1994) demonstrate that a large differential rotation rate within the meddy core is possible, they do not directly help us estimate the value of b for Meddies 1 and 2. Therefore, we will simply assume that the appropriate model parameter values for these meddies are $b \approx 1$ [using (8) it can be shown that when $b = 1$ the velocity field is characterized by a four-fold variation in rotation rate over the depth of the core]. This will provide a near-upper bound on the lens propagation speed for a given background shear. Choosing D and α_* as above, it follows that the predicted translation speed is 0.2 cm s^{-1}. This is significantly smaller than the average observed propagation speed of 1.4 cm s^{-1}. Presumably additional physical effects (e.g., Beckmann et al. 1989; Colin de Verdiere 1992) play a role in producing the observed translation.

6. Float tracking errors

Given the small horizontal displacements of the rotation axes that were observed, especially for Meddy 2, it is natural to question the accuracy of the computed float positions. This is a complex issue because a variety of random and systematic errors could contaminate the position data. The accuracy of absolute position fixes typically depends upon where the float is located with respect to the array of moored autonomous listening stations (ALSs) tracking it, the accuracy of float and ALS clocks, the accuracy of ALS positions, and the accuracy of the mean speed of sound used in the calculations. Mooring motions and sound speed fluctuations will also cause inaccuracies.

The accuracy in determining the relative displacement between two nearby floats is significantly better than the absolute accuracy of a position because several

systematic errors tend to cancel. The positions of each pair of floats in the meddies were calculated the same way, using the same ALSs, the same speed of sound, etc. The size of random errors in the instantaneous displacement between float pairs was estimated to be around 1 km, based on an analysis of the random errors of the float-clock corrections about the mean clock-drift. The clock corrections are related to position errors through variations in the speed of sound. The effect of such random positioning errors is reduced in the analysis, since each point in a low-passed trajectory represents an average over many individual positions. The random error associated with the filtered displacements was estimated to be ~0.18 km for Meddy 2, by applying the filter used for the floats in Meddy 2 to a Gaussian white noise signal with unit variance.

The main systematic differences between float pairs in each meddy were: 1) the slightly different times of signaling (a 20-minute difference for Meddy 2, a 3-hour difference for Meddy 1), 2) slightly different depths (~100 m separation), and 3) loops of different radii (Table 1). These last two differences could result in systematic errors in position and hence spurious results. As described below, we conclude that these systematic errors are smaller than the observed signal or in the wrong direction to account for the observed tilt. We are somewhat tentative about this conclusion, however, because there could be subtle, unknown systematic errors arising from the complicated three-dimensional paths of sound in warm meddies (see Mal'tsev et al. 1990).

We discuss below three possible systematic errors: the first is due to different radii of float loops in Meddy 2 coupled with its warm salty core; the second is due to the different depths and temperatures of floats in the lower part of Meddy 1; the third is due to the different depths of floats, coupled with the vertical gradient of sound speed outside the meddies. We estimate systematic errors by calculating the apparent difference in range between a float and a listening station caused by a difference in sound speed. We then estimate the apparent geographical displacement of a float caused by a sound speed difference, given the tracking configuration used for the meddy floats. Finally, we use a ray-tracing technique to calculate the effect of a float at different positions in a meddy, which is in conditions similar to those found in the Canary Basin.

First, consider the increased sound speed within a meddy core relative to that outside. If two floats are at different radii, sound from the float closer to the meddy axis will (on average) travel through more of the warm water in the core, leading to a decreased net travel-time. The travel-time decrease will be erroneously interpreted as a lateral shift toward an ALS of the more central float relative to the one with larger radius, which could lead one to conclude that the core is tilted. This effect is illustrated in Fig. 8 for the extreme case in which one float is in the center and the other is at the

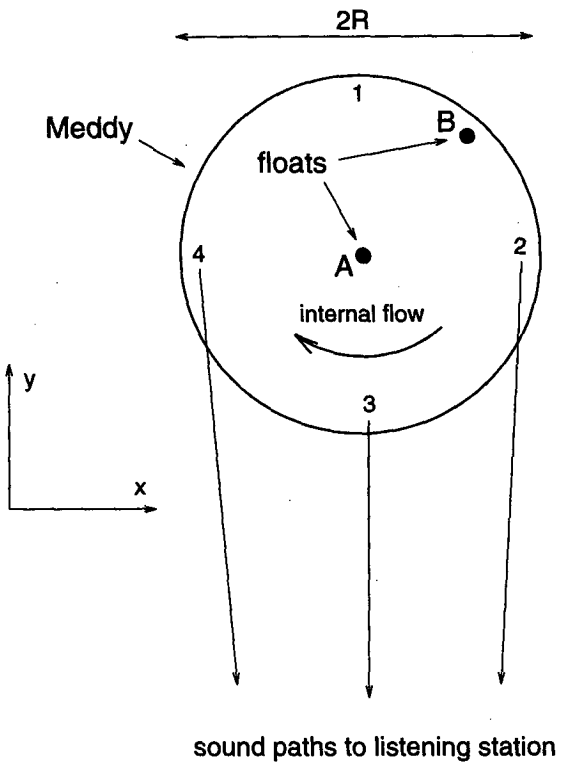

FIG. 8. Mechanism by which results may be biased if the floats are at different radii. Float B passes through points 1, 2, 3, and 4 in the course of a single rotation, while float A stays near the center of the meddy. On average, the sound from float A travels through more of the warm core water than does that from float B, which leads to a travel-time difference and an apparent shift in the relative positions of the two floats. It is estimated that the maximum position error due to this effect is approximately 0.15 km, but in the opposite direction to the tilt observed in Meddy 2.

periphery of the meddy core. At point 1, the sound from float 1 must travel through the full diameter of the meddy to reach the listening stations, while at points 2, 3, and 4, the sound misses the warm core water almost entirely. On average, then, the sound from this float travels a distance of about $\frac{1}{2}R$ through the core, while that from the second float travels a distance R through the core. The *maximum* travel time difference due to this effect is then

$$\Delta t \leq \frac{1}{2} R \left(\frac{1}{c_{\text{outside}}} - \frac{1}{c_{\text{inside}}} \right), \qquad (16)$$

where R is the radius of the core (about 20 km). The maximum deviation in float position due to this effect is, therefore,

$$\Delta R = c\Delta t \leq \frac{1}{2} R \frac{c_{\text{inside}} - c_{\text{outside}}}{c}. \qquad (17)$$

If we assume that the temperature is 10°C inside the core, 6°C outside the core, that the salinity is 36 psu

inside, 35 psu outside, and that the depth is 1100 m, it follows that

$$c_{\text{inside}} \approx 1508 \text{ m s}^{-1} \quad (18)$$

$$c_{\text{outside}} \approx 1494 \text{ m s}^{-1}. \quad (19)$$

The sound speed varies by about 14 m s^{-1} or 1% due to the warm and salty core water. Substituting these values into the expression for ΔR then gives

$$\Delta R \leq 100 \text{ m}. \quad (20)$$

This is significantly smaller than the deviations observed. In addition, since float EB149 in Meddy 2 has smaller radius loops and is shallower than EB148, the direction of the apparent tilt due to this effect is in the opposite direction (southeastward) from that actually observed between EB149 and EB148 (northwestward). We conclude that the observed tilt is not due to this effect.

The two floats below the core of Meddy 1 measured different mean temperatures, 10.0°C at 1121 db and 8.2°C at 1220 db, which corresponds to a difference in sound speed of around 5 m s^{-1}. Over the radius of a 25-km meddy a float whose signal traveled with a 5 m s^{-1} faster sound speed would appear to be ~80 m closer to an ALS, since the signal would arrive earlier. This is likely to be an overestimate because sound rays do not travel horizontally at a constant velocity but are refracted in the deep sound channel. Thus, the average sound speed encountered by a ray is an average of speeds in the sound channel, including the minimum in speed near the axis of the sound channel. Because of this error's small size, we conclude that it does not cause the observed tilt of Meddy 1, although it is in the same general direction as the observed tilt.

The vertical gradient in sound speed outside of meddies is around 0.5 m s^{-1} per 100 db near a pressure of 1100 db (Crouch and Osborne 1981). At typical ranges of 500 km this sound speed gradient implies that a float at 1024 db (Meddy 2) would appear to be ~170 m closer to an ALS than a float at 1129 db. Again, this could be an overestimate because sound rays are refracted vertically in the deep sound channel. Using the actual configuration of ALSs that tracked Meddy 2, we estimate that a float whose signals traveled (at an unknown) 0.5 m s^{-1} faster than that of another float located at the same position would appear to be shifted 250 m toward the southeast relative to the other float. This systematic error is approaching the size of the observed tilt of Meddy 2, but it is in the wrong direction to account for the observed tilt, which is toward the northwest. If somehow the signal from the shallow float of the pair encountered a slower mean speed than the deeper float, then this error would be in the right direction. However, the vertical temperature gradient outside of the meddy implies that the shallow float signal would encounter a faster mean speed, so this scenario seems unlikely.

Acoustic raytraces

We next investigate float positioning errors by using detailed, range-dependent acoustic raytraces. In doing this, we use the high precision multiple profile program (MPP) code originally developed by C. Spofford ("The Bell Laboratories multiple-profile ray-tracing program," informal report). This code is primarily adapted to tomographic applications, giving ray arrival time structures accurate to a few milliseconds. The raytrace study allows us to examine some of the "fine structure" details of what meddies do to the acoustic signal one tracks; that is, produce changes in the multipath arrival structure which, given the limited acoustic bandwidth used in float work, translate into range errors. We are most interested in seeing whether such errors are random or systematic, and what their magnitude is.

In performing this study, we concentrated solely on Meddy 1 because we have detailed hydrographic data for this meddy. We constructed the sound speed profile for the acoustic propagation calculations by taking the meddy (centered at zero km range) to be a perturbation to the winter climatological sound speed profile in the Canary Basin. Sound propagation was calculated from the float sources, located at various depths and ranges within the meddy, to a receiver taken to be at 500 km from the meddy center and at 1200-m depth. For a consistency check, all raytraces were run with and without the meddy. Two main questions were addressed with the raytraces. First, we asked what the effect of source depth is within the meddy. To answer this, we examined the raytraces for floats in the center of the meddy (where the effect would be largest) at depths of 1090, 1120, 1240, and 1300 m. Then, we asked what the effect of source depth is versus range across the meddy. For this study, we used two float depths (1120 and 1240 m) and seven positions (±15 km, ±10 km, ±5 km, and 0 km) across the meddy in the radial direction toward the receiver from the meddy center.

The raypaths and their arrival times are shown in Fig. 9. The first result of interest in the figure is that the raytraces without the meddy generally show *more* acoustic arrivals than the raytraces with the meddy. (This is a well-known result in acoustic tomography: the "simple" ocean generally allows more paths, due to its symmetry, than one perturbed by an eddy or other structure.) The rays that originate in the meddy take longer to reach the source by about 0.2 s on average. This seemingly contradicts the "warmer eddy ⇒ faster travel time" argument posed before. However, that argument presumes that the acoustic paths are completely unperturbed by the meddy, whereas in reality the paths *are* disturbed for the sources in the meddy. The rays

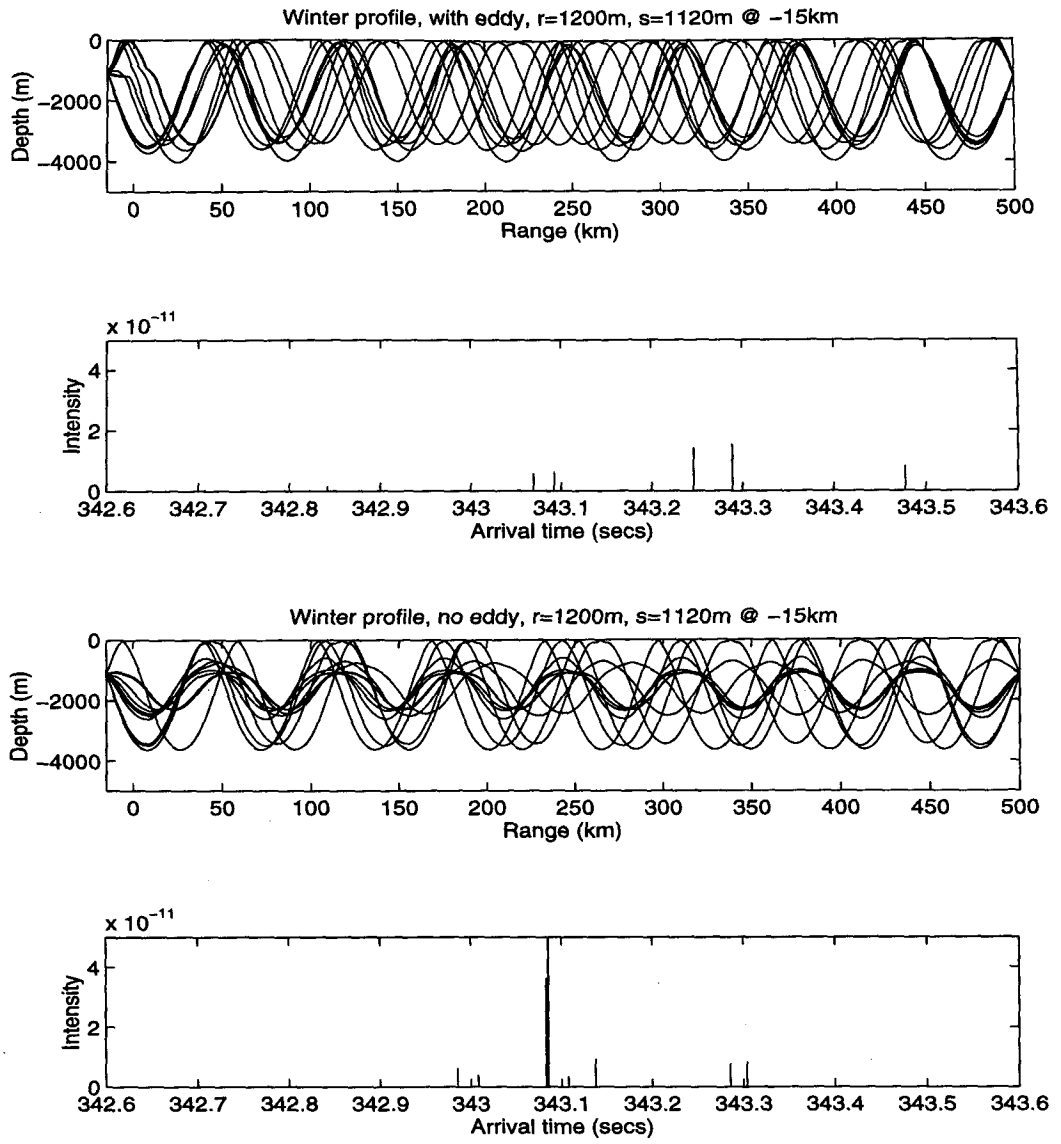

FIG. 9. Raytraces with and without a meddy, with all other parameters (source/receiver depth, range, background soundspeed profile) being held constant. Change in the basic raypath structure is evident both in the raytraces and the arrival time "stick diagrams."

perturbed by the meddy take longer (higher angle) paths in general, and due to the specific interplay of the soundspeed profile and the raypaths for this case, arrive later. Though there is this travel time bias due to the meddy in general, the "debiased" arrival time behavior versus range or depth in the meddy seems to be random, with about a 0.25 sec standard deviation. Thus, we see that the meddy scatters the acoustic energy to higher angles in general, but with no strong dependence on the source position within the meddy. The physical picture is that the rays that propagate through the meddy tend to arrive later and in a more spread out pattern than would be the case if the meddy were not present. Moreover, the most intense arrival of a group of multipath arrivals that has traveled through the meddy is hard to predict, as the intensity fluctuates rather strongly as a function of source position in the meddy. Thus, the arrival the processor picks has what is essentially a *random* error of about a half-second (± 0.25 sec) due to the "medium fluctuations" effect and about a 0.2 sec slow bias. Since the slow bias is not important to the difference in arrival times for float pairs in a meddy and since random errors tend to be averaged out by the low-pass filter used in the analysis,

we conclude that there is no systematic error associated with sound transmission in meddies that would account for the observed tilts.

7. Discussion

Rossby (1988) and Schultz Tokos et al. (1994) have previously reported observations of tilting meddies. These authors observed periodic pressure modulations in meddy float trajectories, which were considered to be the signature of the geostrophic flow in the vicinity of the meddies. They used the pressure data to infer isopycnal slopes in the core region, and interpreted these slopes as representing geostrophic flow velocities relative to quiescent waters deeper down. In this manner, Rossby calculated a velocity of 2 cm s^{-1} for Meddy Sharon (which we refer to as Meddy 1), while Schultz Tokos et al. computed a velocity of over 8 cm s^{-1} for one of a pair of meddies that were found to be rotating about a common center. These computed velocities were in good agreement with observed translation velocities for the meddies. Velocities of 2 cm s^{-1} or greater are large compared to mean flow speeds at these depths, which may indicate that a significant fraction of the observed isopycnal slope in these meddies is a result of the dynamical response of the meddies to the external shear. However, it is unclear what role the induced slopes (and the associated velocities) play in the translation of the meddies.

In terms of our model representation, the interpretations of Rossby and Schultz Tokos et al. are equivalent to assuming that meddies move at speeds roughly equal to the maximum speed of the large-scale flow field impinging on the core, assuming large-scale flow velocities beneath the meddies are very slow. Such a scenario allows for a bulk advection by the external flow because the mean background velocity over the core region need not vanish. This effect was not considered in our analysis since it was our intention to explore the possibility of a hetonlike propagation mechanism for meddies, but it may be a reasonable representation of the conditions actually "seen" by meddies in the ocean. In addition, this interpretation seems consistent with recent theoretical work by Dewar and Meng (1995), who represent meddies as homogeneous lenses "sandwiched" between homogeneous upper and lower layers and conclude that meddies move at a density-weighted average of the flow velocities in the upper and lower layers.

It is worth noting that Rossby's estimate of the isopycnal slope inside Meddy 1, along with the model results discussed in this work, can be used to infer the strength of the vertical shear in which the meddy was embedded. To do this, we use the thermal wind and hydrostatic equations to derive an expression relating vertical shear and isopycnal slope:

$$u_z = \frac{N^2}{f}\left(\frac{\partial z}{\partial y}\right)_\rho . \qquad (21)$$

After accounting for the different compressibilities of floats and seawater, Rossby (1988) estimated that water parcels moved vertically by about 15 m as they went from one side of the meddy to the other (a horizontal distance of 30 km). This implies an isopycnal slope of 15 m/30 km $\sim 5 \times 10^{-4}$ across the meddy core. Thus, using $f = 7 \times 10^{-5}$ s^{-1}, $N = 2.5 \times 10^{-3}$ s^{-1}, and $(\partial z/\partial y)_\rho = 5 \times 10^{-4}$, we obtain a value of $u_z = 4.5 \times 10^{-5}$ s^{-1} for the shear *inside* the meddy core. This is not equal to the large-scale shear outside the core because, according to the discussion in section 5, we expect that the meddy's dynamical response will cause the vertical shear in the core (and hence also the isopycnal slope) to differ from background values. In section 5 it was shown that for a meddy with core radius $R = ND/f$ the vertical shear u_z in the core is larger by a factor of $2^1/_2$ than the background vertical shear. Thus, our best estimate of the shear outside Meddy 1 is $^1/_{2.5} \times 4.5 \times 10^{-5}$ $s^{-1} = 1.8 \times 10^{-5}$ s^{-1}, which is in reasonably good agreement with the value of 2.5×10^{-5} s^{-1} we inferred from the hydrographic sections of Saunders (1981).

8. Conclusions

We conclude that the float data show a tilt of the rotation axes of two different meddies. The observed tilts are attributed to a combination of kinematical and dynamical effects. The kinematic tilts are a result of the superposition of the meddy velocity field, the external vertical shear, and the translation velocity of the meddy, while the dynamical tilting results from the secondary flows associated with the deformation of the meddy core by external flows.

The size of the observed tilt of Meddy 2 ($\sim$0.4 km over $\sim$100 m depth) is consistent with a variation in external flow speed of about 2 cm s^{-1} over the depth of the core, and the sense of the tilt is consistent with an external flow that is approximately parallel to the drift direction of the meddy, which becomes faster near the surface. A background shear of this magnitude is consistent with the available data concerning the vertical structure of flow within the Canary Basin. Thus, the displacements measured for Meddy 2 appear to represent a deformation of the meddy core by vertically sheared flow outside the meddy. The observed displacements were much larger for Meddy 1 ($\sim$6 km over $\sim$100 m depth); we conclude that this is because the floats were not in the core but were instead in the region of trapped fluid beneath the core. The large displacements observed for Meddy 1 can be understood by considering the combined effects of the depth-dependent rotation rate beneath the core and the horizontal translation of the meddy. The sense of the predicted movement of the model eddy is in qualitative agreement with the observed meddy translation for both meddies, but the observed speeds are significantly larger than predicted by the model. Apparently the

meddy deformations are adequately reproduced by the simple model discussed here, but additional physical effects [such as those discussed by Beckmann et al. (1989) and Colin de Verdiere (1992)] play a role in the translation of the meddies.

While the float data concerning meddy tilt seem very clear (Figs. 3 and 4), we think the results are more suggestive than definitive. This is because of our subjective choice of trajectories to study and the rather small relative displacements of floats in Meddy 2. We have investigated position errors and concluded that they are smaller than the relative float displacements, and in several cases in the opposite direction to the observed tilt. Although acoustic propagation in an inhomogeneous ocean is complicated and unknown systematic acoustic effects could lead to additional apparent differences in the positions of floats at different depths and radii within a meddy, acoustic raytracing through a model meddy does not reveal any systematic error that could account for the observed displacements.

Acknowledgments. Funds were provided by National Science Foundation Grants OCE-9009463 and OCE-9301234. During the initial stages of this work D. Walsh was supported by National Science Foundation Grants OCE-891 6446, OCE-911 5359, OCE-87-00 601, and by the Office of Naval Research Grant N 00014-89-J-1182. The floats were tracked by M. Zemanovic and C. Wooding. We thank Arthur Newhall for helping out with the raytracing calculations.

REFERENCES

Armi, L., and W. Zenk, 1984: Large lenses of highly saline Mediterranean water. *J. Phys. Oceanogr.*, **14,** 1560–1576.

——, D. Hebert, N. Oakey, J. Price, P. L. Richardson, T. Rossby, and B. Ruddick, 1989: Two years in the life of a Mediterranean salt lens. *J. Phys. Oceanogr.*, **19,** 354–370.

Beckmann, A., and R. H. Käse, 1989: Numerical simulation of the movement of a Mediterranean salt lens. *Geophys. Res. Lett.*, **16,** 65–68.

Colin de Verdiere, A., 1992: On the southward motion of Mediterranean salt lenses. *J. Phys. Oceanogr.*, **22,** 413–420.

Crouch, J. H., and K. R. Osborne, 1981: Atlantic Ocean/ASEPS sound speed profiles, Colborn-analyzed watermass data base. Final Technical Task Report, Ocean Data Systems Inc., San Diego, 101 pp.

Dewar, W. K., and H. Meng, 1995: The propagation of submesoscale coherent vortices. *J. Phys. Oceanogr.*, **25,** 1745–1770.

Flierl, G. R., 1981: Particle motions in large amplitude wave fields. *Geophys. Astrophys. Fluid Dyn.*, **18,** 39–74.

——, V. D. Larichev, J. C. McWilliams, and G. M. Reznik, 1980: The dynamics of baroclinic and barotropic solitary eddies, *Dyn. Atmos. Oceans,* **5,** 1–41.

Hebert, D. L., 1988: A Mediterranean salt lens. Ph.D. thesis, Dalhousie University, 187 pp.

Hogg, N. G., and H. M. Stommel, 1990: How currents in the upper thermocline could advect Meddies deeper down. *Deep-Sea Res.*, **37,** 613–623.

Mal'tsev, N. E., K. D. Sabinin, and A. V. Furduev, 1990: Acoustical and oceanographic experiment at the lens of Mediterranean waters of the Atlantic Ocean. *Sov. Phys. Acoust.*, **36**(1), 46–50.

McWilliams, J. C., 1985: Submesoscale coherent vortices in the ocean. *Rev. Geophys.*, **23,** 165–182.

Prater, M. D., and T. B. Sanford, 1994: A meddy off Cape St. Vincent. Part I: Description. *J. Phys. Oceanogr.*, **24,** 1572–1586.

Press, W. H., B. P. Flannery, S. A. Teukolsky, and W. T. Vetterling, 1986: *Numerical Recipes—The Art of Scientific Computing.* Cambridge University Press, 818 pp.

Price, J. F., T. K. McKee, J. R. Valdes, P. L. Richardson, and L. Armi, 1986: SOFAR float Mediterranean outflow experiment data from the first year, 1984–1985. Woods Hole Oceanographic Institution Tech. Rep. WHOI-86-31, 204 pp.

Richardson, P. L., D. Walsh, L. Armi, M. Schröder, and J. F. Price, 1989: Tracking three meddies with SOFAR floats. *J. Phys. Oceanogr.*, **19,** 371–383.

——, M. S. McCartney, and C. Maillard, 1991: A search for meddies in historical data. *Dyn. Atmos. Oceans,* **15,** 241–265.

Rossby, T., 1988: Five drifters in a Mediterranean salt lens. *Deep-Sea Res.*, **35,** 1653–1663.

Saunders, P. M., 1981: Circulation in the eastern North Atlantic. *J. Mar. Res.*, **40,** 641–657.

Schultz Tokos, K. L., and T. Rossby, 1991: Kinematics and dynamics of a Mediterranean salt lens. *J. Phys. Oceanogr.*, **21,** 879–892.

——, H. Hinrichsen, and W. Zenk, 1994: Merging and migration of two meddies. *J. Phys. Oceanogr.*, **24,** 2129–2141.

Walsh, D., 1992: A model of a Mediterranean salt lens in external shear. Ph.D. thesis, Woods Hole Oceanographic Institution/Massachusetts Institute of Technology Joint Program in Oceanography, 168 pp.

——, 1995: A model of a mesoscale lens in large scale shear. Part I: Linear calculations. *J. Phys. Oceanogr.*, **25,** 735–746.

Zemanovic, M. E., P. L. Richardson, J. R. Valdes, J. F. Price, and L. Armi, 1988: SOFAR Float Mediterranean Outflow Experiment Data from the second year, 1985–1986. Woods Hole Oceanographic Institution Tech. Rep. WHOI-88-43, 234 pp.